Am J Transl Res 2023;15(7):4887-4901
www.ajtr.org /ISSN:1943-8141/AJTR0150047

Original Article

Progranulin modulates the progression of non-small cell lung cancer through lncRNA H19

Biao Gu[1,2], Maoyuan Yang[1], Liang Shi[1], Guangda Yuan[1,3], Hongya Xie[1,3], Bin Ni[1]

[1]Department of Thoracic Surgery, The First Affiliated Hospital of Soochow University, 899 Pinghai Road, Suzhou 215006, Jiangsu, China; [2]Department of Thoracic Surgery, The Affiliated Huai'an No. 1 People's Hospital of Nanjing Medical University, 1 Huanghe West Road, Huai'an 223300, Jiangsu, China; [3]Department of Thoracic Surgery, The Affiliated Suzhou Hospital of Nanjing Medical University, 16 Baita West Road, Suzhou 215006, Jiangsu, China

Received March 8, 2023; Accepted June 1, 2023; Epub July 15, 2023; Published July 30, 2023

Abstract: Objective: This study aimed to explore the specific mechanism of action of Progranulin (PGRN) in non-small cell lung cancer (NSCLC) and its interaction with lncRNA H19. Methods: Normal and cancerous lung tissues were collected from patients with NSCLC and healthy volunteers. We assessed the expression of PGRN in both groups using immunohistochemistry, quantitative-reverse transcription-polymerase chain reaction (qRT-PCR), and western blotting (WB). Results: Compared to the controls, PGRN expression was noticeably higher in tumor tissues. The high expression of PGRN in patients with NSCLC was inversely correlated to the prognosis and strongly associated with the biological features and clinicopathologic data. High PGRN expression significantly improved the ability of NSCLC cells to proliferate and migrate and was positively correlated with tumor formation, based on in vitro and in vivo cellular tests. Expression of lncRNA H19 was also found to be elevated in NSCLC tissue and cells. The expression of H19 was correlated with tumor growth in vivo and in vitro, and H19 regulated PGRN by mediating the expression of miR-29b-3p. Conclusions: H19 and PGRN can serve as biomarkers and therapeutic targets in NSCLC.

Keywords: Non-small cell lung cancer, H19, miR-29b-3p, progranulin (PGRN), proliferation

Introduction

Lung cancer is the leading cause of cancer-related death worldwide. Histologically, there are two main subtypes of lung cancers, small cell lung cancer and non-small cell lung cancer (NSCLC), with the former accounting for approximately 15% of all cases, and the latter accounting for about 85% [1]. Treatments targeting biological changes have considerably improved patient response, with a 5-year survival rate of 10.15%. Upon diagnosis, 40% of patients are found to have stage IV lung cancer. This necessitates finding new targets for the diagnosis and treatment of NSCLC [2, 3].

Progranulin (PGRN) is a pleiotropic growth factor that mediates cell cycle progression and motility. It also functions as a glucose glycoprotein and regulates cell growth, migration, and transformation as well as the cell cycle, wound healing, tumorigenesis, and cytotoxic drug resistance [4-6]. Additionally, rapidly expanding tumor tissues have high levels of PGRN, which worsens the malignancy. This protein also promotes tumor proliferation and development of other related diseases, such as gastric cancer, breast cancer, cervical cancer, colorectal cancer, kidney injury, neurodegeneration, neuroinflammation, human atherosclerotic plaques, liver cancer, and acute kidney injury [7-9]. PGRN expression was observed to be increased in *Helicobacter pylori*-infected human gastric cancer epithelial cell lines SGC 7901 and GES-1 [10]. PGRN infection significantly enhanced the invasive metastasis of gastric cancer cells. Interference with PGRN significantly reduced cell proliferation and migration induced by *H. pylori* infection. Chen et al. suggested that PGRN exacerbated the progression of NSCLC through PI3K/AKT/Bcl-2 anti-apoptotic signaling [11]. However, they demonstrated the effect of PGRN only in H520 cells, a lung squamous cell carcinoma cell line.

Table 1. Clinicopathologic data of patients with non-small cell lung cancer

Variable	Number of patients
Age	
≥ 60	38
≤ 60	12
Sex	
Male	36
Female	14
Smoking history	
Yes	43
No	7
Pathologic classification	
Adenocarcinoma	25
Squamous carcinoma	22
Other	3
T-stage	
T1	14
T2	21
T3	15
TNM staging	
I	13
II	16
III	14
IV	7
N phase	
N0	10
N1	17
N2	12
N3	11

Zhou et al. reviewed the functions of PGRN in various cancers. They concluded that several signaling pathways and molecules are involved in the effects of PGRN on cancer cells, including Akt, mitogen-activated protein kinase (MAPK), vascular endothelial growth factor (VEGF), and cyclin D1. Therefore, PGRN is a possible diagnostic and prognostic biomarker for cancers and a possible target for anticancer therapy [12]. Although the mechanism of PGRN molecular transition across lung cancer is better understood, further investigation is required to explore its applicability to NSCLC and its mechanism of action.

A recently identified class of non-coding RNAs called long-stranded non-coding RNAs (lncRNAs) can participate in multilevel fine regulation of tumor cell proliferation, migration, and apoptosis [13, 14]. lncRNAs are defined as non-protein-coding RNA transcripts longer than 200 nt [15-17]. By interacting with proteins and miRNA targets, lncRNAs can regulate gene expression and signaling pathways at the epigenetic, transcriptional, and post-transcriptional levels [17]. It has been shown that lncRNAs are involved in the process of NSCLC development and progression, and lncRNA H19 was found to regulate the resistance of lung cancer cells to cisplatin-based chemotherapeutic drugs [18]. H19 is aberrantly expressed in a variety of malignant tumors and plays an important role in tumor development, particularly in metastasis and invasion. H19 can be used for early molecular diagnosis, targeted therapy, and prediction of the efficacy and prognosis in patients with lung cancer. H19 is substantially associated with the occurrence, development, distant metastasis, and prognosis of lung cancer [19]. The level of H19 is much higher in lung cancer tissue than in healthy tissue near the tumor. H19 overexpression may increase the invasion and proliferation of lung cancer cells by encouraging epithelial- mesenchymal transition [20].

We speculate that PGRN may be related to the prognosis of NSCLC patients and that the growth of NSCLC lncRNA H19 may regulate the expression of PGRN, which in turn may mediate the development of NSCLC. In this study, surgically resected lung cancer tissue from patients with NSCLC and normal lung tissue obtained by wedge pneumonectomy were collected from patients with NSCLC. The expression of PGRN was compared among patients at different TNM stages to analyze the relationship of PGRN with the prognosis in NSCLC. The effects of PGRN on NSCLC development were investigated using functional assays.

In this study, we investigated the regulatory effect of the H19/miR-29b-3p/PGRN axis on NSCLC development and employed various cell functional assays to explore the mechanism by which H19 mediates NSCLC development through regulating miR-29b-3p and PGRN.

Materials and methods

NSCLC tissue specimens

TNM staging was determined based on postoperative pathology with reference to the *International TNM Staging 8th edition* (**Table 1**).

Tumor specimens were obtained from 50 patients with NSCLC who underwent surgical treatment at the Department of Thoracic Surgery of the First Affiliated Hospital of Soochow University between September 2018 and September 2021. All tissue specimens, including lung cancer and healthy lung tissues, were frozen in liquid nitrogen and then placed in a refrigerator at -80°C. This study was approved by the Ethics Committee of First Affiliated Hospital of Soochow University. Informed consent was obtained from all patients for all experiments.

Immunohistochemical detection of PGRN expression in lung tissue

To determine the expression of PGRN protein in NSCLC and normal lung tissues, we performed qualitative localization, and semi-quantitative examinations in tissue samples using immunohistochemical techniques. Briefly, tumor samples were fixed in 4% formaldehyde, embedded in paraffin, and then sliced into 5-μM sections. Samples were deparaffinized in xylene and rehydrated. After blocking endogenous peroxidase and performing antigen retrieval, tissue slices were blocked in goat serum for 30 min and incubated with antibodies against PGRN (1:100 dilution, Santa Cruz, Santa Cruz, CA, USA) overnight at 4°C, followed by incubating with biotinylated secondary antibody (Santa Cruz) for 30 min. Staining was performed in parallel using the Vectastain ABC kit (Vector Laboratories, Burlingame, CA, USA).

Cell culture

The NSCLC cell line A549 was cultured in high-sugar medium. Adherent cells were cultured in media containing 10% fetal bovine serum (FBS). The medium was changed every 2 d, and the cells were trypsinized when confluence reached 80-90%. After being treated with medium containing 10% FBS, the medium of bovine serum was centrifuged at 1000 rpm for 10 min after the digestion. The medium was then discarded, and the cell pellet was retained and resuspended in medium containing 10% FBS before being passaged at a ratio of 1:3 to continue the culture.

Grouping information

To evaluate the effect of PGRN in A549 cells, loss- and gain-of-function experiments were performed. The cells were divided into three groups: negative control group (NC, no treatment), PGRN overexpression group (oePGRN, cells were transfected with PGRN overexpression vector), and PGRN silencing group (cells were transfected with PGRN siRNA).

To evaluate the effect of H19 in A549 cells, the loss- and gain-of-function experiments were performed. The cells were divided into four groups: overexpression control group (oeNC, cells were transfected with empty vector), H19 overexpression group (oeH19, cells were transfected with H19 overexpression vector), siRNA-negative control group (siNC, cells were transfected with siRNA-negative control), and siRNA-H19 group (cells were transfected with siRNA-H19).

Quantitative reverse transcription-polymerase chain reaction (qRT-PCR)

qRT-PCR was performed as previously described [21]. Briefly, total RNA was extracted from tissues or cells using the TRIzol reagent (Invitrogen, Carlsbad, CA, USA). qRT-PCR analysis of PGRN mRNA was performed using QIAGEN OneStep RT-PCR kit (Qiagen, Valencia, CA, USA). GAPDH was used as an internal control.

To measure H19 and miR-29b-3p expression, total RNA was polyadenylated and reverse transcribed using the TaqMan MicroRNA Reverse Transcription Kit and TaqMan miRNA assay (Applied Biosystems, Foster City, CA, USA) based on the manufacturer's instructions. U6 small nuclear RNA served as an internal control.

qRT-PCR was performed in triplicate. Relative expression of the tested genes was calculated and normalized using the $2^{-\Delta\Delta Ct}$ method. Primers were as follows: PGRN F, 5'-ATG TGG GTC CTG ATG AGC TG-3', R, 5'-GCT CGT TAT TCT AGG CCA TGT G-3'; GAPDH F, 5'-GCA CCG TCA AGG CTG AGA A-3', R, 5'-TGG TGA AGA CGC CAG TGG A-3'; H19 F, 5'-CTC AAA CGA CAA GAG ATG GT-3', R, 5'-AGT GTA GTG GCT CCA GAA TG-3'; miR-29b-3p F, 5'-TAG CAC CAT TTG AAA TCA GTG TT-3', R, 5'-CCA GTG CAG GGT CCG AGG T-3'; U6 F, 5'-CTC GCT TCG GCA GCA CA-3', R, 5'-AAC GCT TCA CGA ATT TGC GT-3'.

Cell counting kit-8 (CCK-8) assay

Well-grown cells in the logarithmic growth phase were collected. The cells were washed

twice in phosphate-buffered saline (PBS) buffer, and the cell suspension was diluted to 3000 cells/100 μL based on the cell density. The diluted cell suspension was seeded to a 96-well culture plate at 3000 cells per well. After culturing for approximately 6-8 h, the cells adhered, and 10 μL of CCK-8 reagent was added to the 96-well culture plate based on a ratio of CCK-8: medium = 1:9. Incubation was continued for 2 h, and the absorbance value (optical density, OD) of each well at 450 nm was measured using an enzyme marker. The OD values were measured continuously for 0 h (that is, 6-8 h after cell adhesion), 24, 48, and 72 h. The proliferative ability of each group of cells was assessed based on OD values.

Wound healing assay

The cell suspensions were prepared using logarithmically well-grown cells after digestion. Cells were seeded in 6-well plates at a density of 1-5 × 10^5 cells/well. When the cell growth density was close to 100%, a 200 μL pipette tip was used to create a scratch through the center of the well. After 48 h, the cells were removed from the 6-well plates, photographed under a microscope, and marked at 36 h. The acquired images were analyzed using the ImageJ software to calculate the cell migration rate at 0 and 36 h, respectively.

Transwell assay

Serum-free medium was added to the transwell upper and lower chambers, respectively, and the basement membrane was hydrated for 30 min at 37°C in a 25% CO_2 incubator. Matrigel substrate gel was thawed at 4°C in the refrigerator, diluted with serum-free medium at a ratio of Matrigel substrate gel: medium = 1:8, and spread evenly into the upper chamber of the transwell. The logarithmically grown cells were detached, and about 5 × 10^4 cells were transferred to the upper chamber of the Transwell. Then, 600 μL of complete medium containing 20% serum was added to the lower chamber, and the upper chamber of the Transwell was placed onto the corresponding lower chamber. After incubation for 24 h, the culture solution in the upper chamber was discarded. The chambers were washed twice with PBS buffer, fixed in 4% paraformaldehyde solution for 30 min, and air-dried at room temperature. Transwell chambers were stained with 1% crystal violet solution for 20 min and were observed under a microscope. Five randomly selected fields of view were photographed, and the cells were counted.

Flow cytometry

Approximately 1 × 10^6 cells were resuspended and centrifuged at a speed of 1000 rpm for 5 min in a low-temperature high-speed centrifuge. Then, the cells were added with 5 μl Annexin V-FITC (Fluorescein Isothiocyanate) and 10 μl propidium iodide staining solution, mixed gently, and incubated at room temperature for 20 min in the dark. Subsequently, the samples were placed on ice and tested using a machine.

Subcutaneous tumorigenesis assay in BALB/c nude mice

Four-week-old female BALB/c nude mice were randomly divided into sh-lncRNA H19 and sh-NC groups, with five mice in each group. The mice's rumps were subcutaneously injected with lentivirus-infected cells. The tumor size was measured every 4 d, and the tumor volume was calculated as follows: tumor volume = (length × $width^2$)/2 (mm^3). On day 28, the mice were euthanized, and the tumors were removed, weighed, and photographed. The experimental protocol was approved by the Animal Ethics Committee of First Affiliated Hospital of Soochow University.

Statistical analysis

All data from this study were statistically analyzed using SPSS 22.0. Each experimental group contained at least three replicates. Data were expressed as mean ± standard deviation (SD). $P < 0.05$ was considered statistically significant when comparing data from two groups using the least significant difference t-test, between groups using independent samples t-test, and among several sets of data using one-way ANOVA.

Results

Expression of PGRN in NSCLC tissue and its role in the development of NSCLC

To understand the role of PGRN in NSCLC development, we examined PGRN expression in NSCLC tissues. The qPCR results exhibited that

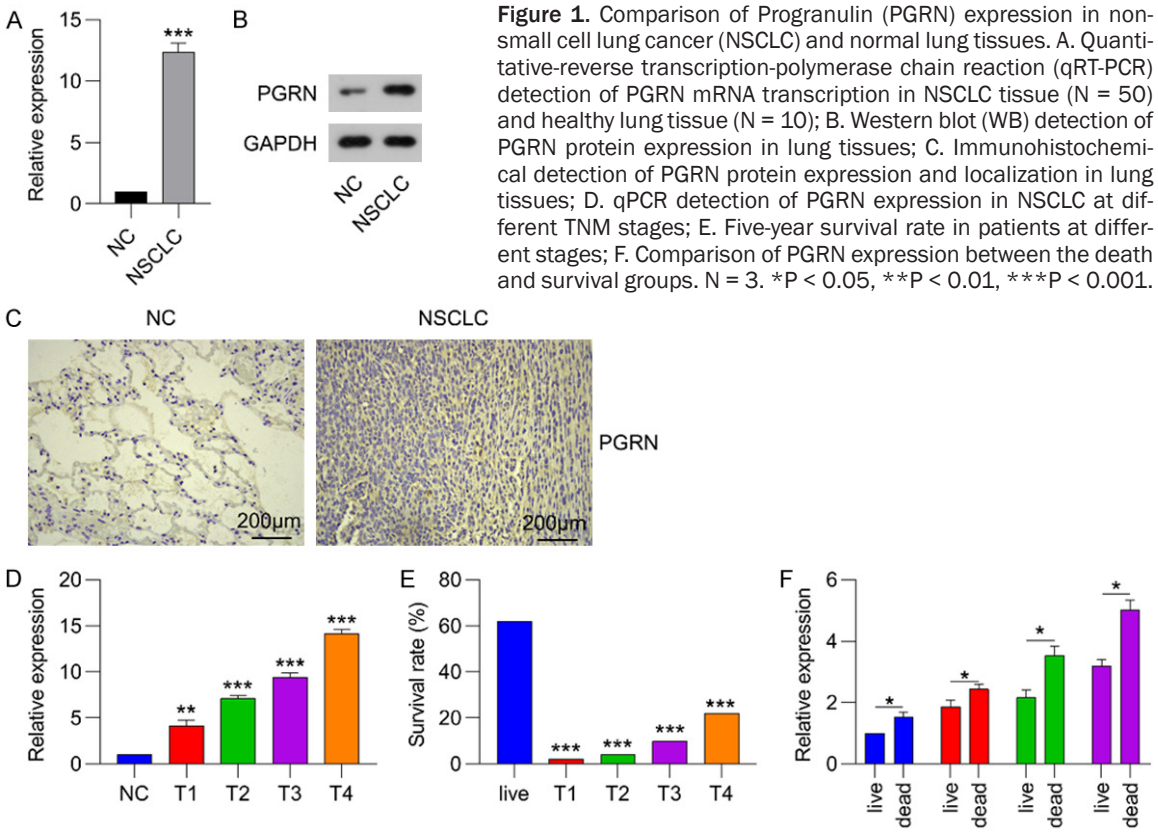

Figure 1. Comparison of Progranulin (PGRN) expression in non-small cell lung cancer (NSCLC) and normal lung tissues. A. Quantitative-reverse transcription-polymerase chain reaction (qRT-PCR) detection of PGRN mRNA transcription in NSCLC tissue (N = 50) and healthy lung tissue (N = 10); B. Western blot (WB) detection of PGRN protein expression in lung tissues; C. Immunohistochemical detection of PGRN protein expression and localization in lung tissues; D. qPCR detection of PGRN expression in NSCLC at different TNM stages; E. Five-year survival rate in patients at different stages; F. Comparison of PGRN expression between the death and survival groups. N = 3. *P < 0.05, **P < 0.01, ***P < 0.001.

the mRNA expression of PGRN was significantly higher in NSCLC tissue than in paraneoplastic tissues (**Figure 1A**). Immunohistochemical staining of tumor specimens and WB showed similarly higher PGRN expression in NSCLC tissue (**Figure 1B** and **1C**).

To investigate whether the expression of PGRN in NSCLC tissue was related to TNM stage, we classified the patients into T1, T2, T3, and T4 stages based on the TNM stage. The expression levels of PGRN mRNA in lung cancer tissue at different stages were detected using qPCR. The results demonstrated that the expression of PGRN mRNA was increased in tumor specimens at each TNM stage compared with that in normal lung tissue, and the higher the TNM stage, the higher the expression of PGRN (**Figure 1D**). These findings imply that PGRN plays a significant role in promoting tumor growth and progression.

To further elucidate the relationship between high PGRN expression, malignant behavior, and the progression of NSCLC, we evaluated the correlation between PGRN expression and the survival of patients. Through a five-year telephone follow-up of the 50 patients with NSCLC, we calculated a 5-year postoperative survival rate of 62%, with 19 patients died within 5 years, including 11 patients (58%) who died at stage IV, 5 patients (26.3%) at stage III, 2 patients (10.5%) at stage II, and 1 patient (5.2%) at stage I. By comparing PGRN expression in tumor tissue of dead and surviving patients at different stages, results of qPCR showed that PGRN expression was higher in dead patients than in surviving patients (**Figure 1E** and **1F**). These results indicate that PGRN expression levels are negatively correlated with the 5-year survival rate of patients with NSCLC.

Expression and role of PGRN in NSCLC A549 cells

To validate these results, we examined the background expression of PGRN in normal bronchial, HBE cells versus NSCLC A549 cells in vitro. qPCR results showed that the expression level of PGRN mRNA was significantly higher in A549 cells than in normal HBE cells (**Figure 2A**). Similarly, WB results exhibited that the expression of PGRN protein was higher in the A549 cells than in the normal HBE cells (**Figure**

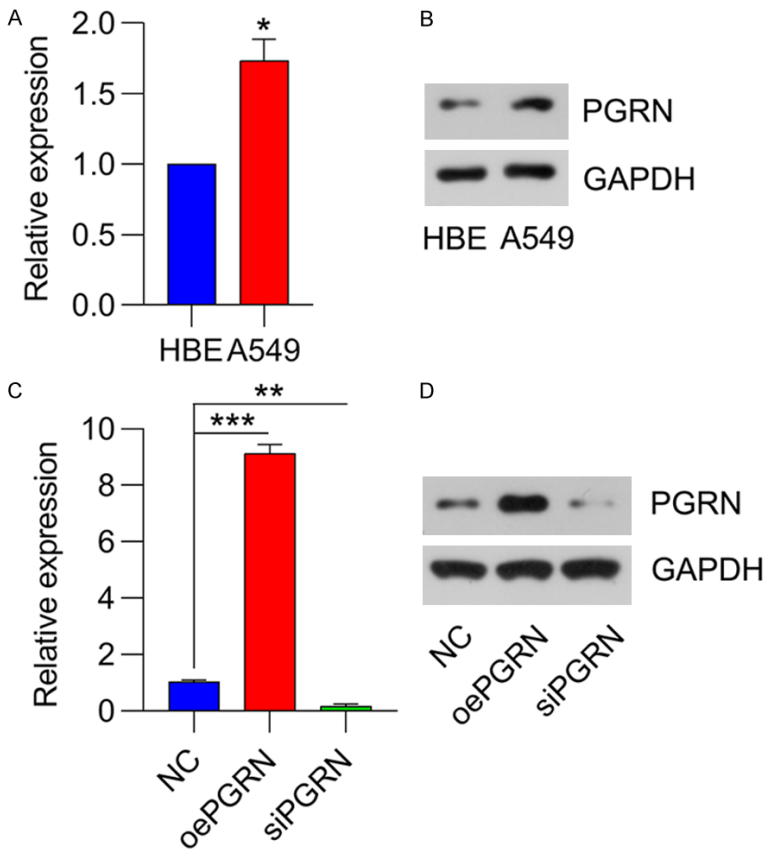

Figure 2. Detection and regulation of PGRN expression in tumor cells. A. qPCR detection of PGRN mRNA levels; B. WB detection of PGRN protein levels; C, D. Construction of A549 cell lines overexpressing or knocking down PGRN. qPCR and WB detection of the target gene PGRN in overexpressed and knocked down cell lines. N = 3. *P < 0.05, **P < 0.01, ***P < 0.001.

2B). High levels of PGRN expression in NSCLC cells further suggested that PGRN plays a crucial role in the development of NSCLC.

PGRN protein expression was negatively correlated with the five-year survival rate of the NSCLC patients. To verify whether the development of NSCLC is associated with PGRN expression, the effects of PGRN expression on the malignant behavior of tumor cells were investigated by lentiviral infection of A549 cells with in vitro overexpression/knockdown of PGRN. The qPCR results showed that the lentivirus carrying the PGRN overexpression gene successfully infected A549 cells (**Figure 2C**) and overexpressed the target gene, PGRN (**Figure 2C**). WB results showed that A549 cells transfected with a lentivirus overexpressing lentivirus PGRN transcribed and translated higher levels of PGRN protein (**Figure 2D**). A549 cells transfected with PGRN knockdown did not transcribe or translate the PGRN protein (**Figure 2C** and **2D**).

Next, we examined the effects of PGRN overexpression or knockdown on the viability and proliferation of NSCLC A549 cells using MTT and CCK8 assays. The results showed that there was no difference in the proliferation and viability between the PGRN overexpression and knockdown groups and the control group at the early cellular stage. After 12 h, the cells in the PGRN overexpression group showed higher proliferation activity, whereas the proliferation activity in the PGRN knockdown group was lower than that of the controls (**Figure 3A** and **3B**). Moreover, clone formation assays and live cell counts revealed a significant increase in the proliferative capacity of PGRN-overexpressing cells, and the number of live cells in the PGRN overexpression group was significantly higher than that in the negative control group. In contrast, the number of viable cells in the PGRN knockdown group was significantly lower than that of the negative control group (**Figure 3C**). The results indicated that increasing PGRN expression promoted the proliferation of A549 cells, and knockdown of PGRN inhibited the proliferation of A549 cells.

Previous experiments confirmed the proliferative effect of PGRN on cell proliferation. We investigated the effect of PGRN on the cell cycle of NSCLC cells by flow cytometry. When PGRN was knocked down, an extended G1 phase was observed (**Figure 3D**), which blocked cell proliferation, illustrating the effect of PGRN on the cell cycle and proliferation.

The primary contributors to the malignant progression of cancer are tumor cell invasion and migration. The results of the wound healing assay showed that the healing time of A549

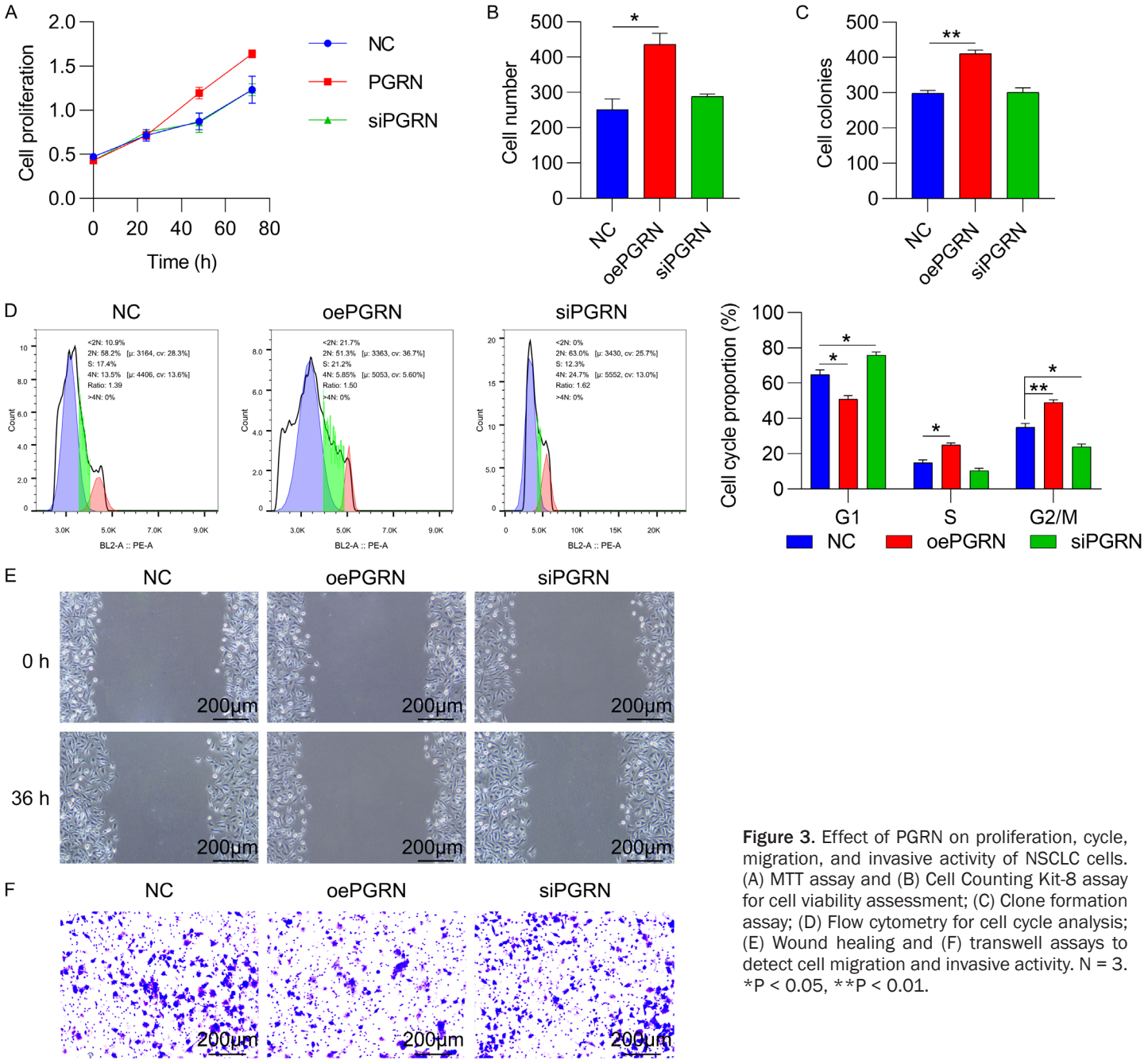

Figure 3. Effect of PGRN on proliferation, cycle, migration, and invasive activity of NSCLC cells. (A) MTT assay and (B) Cell Counting Kit-8 assay for cell viability assessment; (C) Clone formation assay; (D) Flow cytometry for cell cycle analysis; (E) Wound healing and (F) transwell assays to detect cell migration and invasive activity. N = 3. *P < 0.05, **P < 0.01.

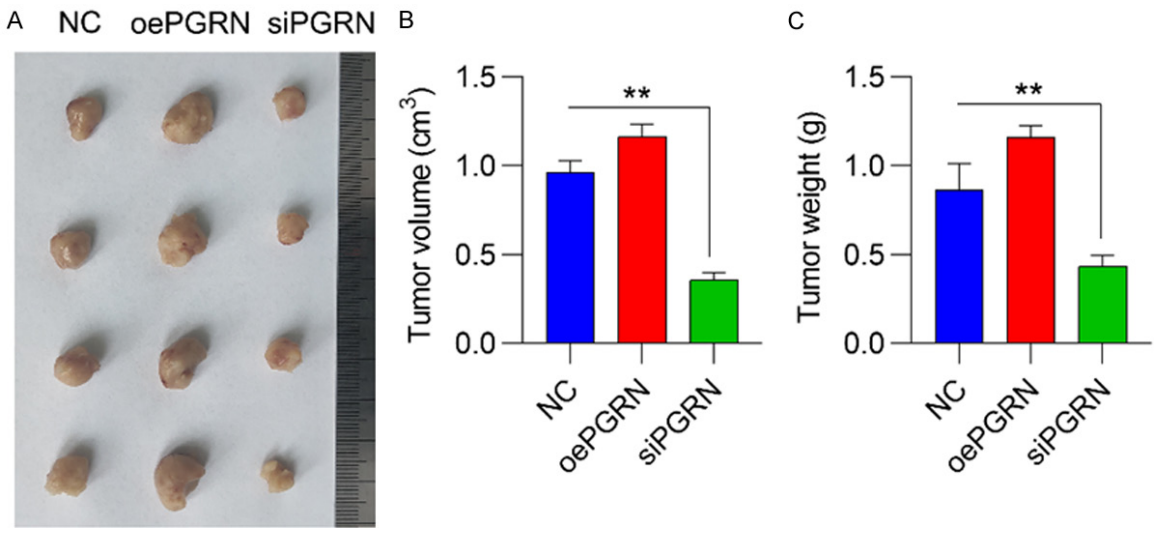

Figure 4. Effect of PGRN on subcutaneous tumorigenic ability of nude mice. Lentiviral constructs of A549 stably transfected cell lines with silenced or overexpressed PGRN negative control were subcutaneously injected into nude mice and examined after tumor formation. A. Representative tumor images; B. Tumor volume at 28 d after transplantation; C. Tumor weight. N = 5. **P < 0.01.

cells in the PGRN overexpression group was significantly shorter than that of the control group, whereas the healing rate of A549 cells in the knockdown group was significantly slower than that of the control group (**Figure 3E**). The transwell assay also showed that the invasion ability of A549 cells in the PGRN knockdown group was significantly weaker than that of the control group during the same time period. In contrast, the invasive ability of A549 cells was significantly enhanced upon PGRN overexpression (**Figure 3F**). These results suggest that PGRN silencing inhibits cell migration and invasion, whereas PGRN overexpression promotes cell migration and invasion, indicating that PGRN promotes the migratory ability of NSCLC cells.

Effect of PGRN on subcutaneous tumorigenic ability in nude mice

We performed in vivo experiments to further verify the effect of PGRN on NSCLC using lentiviral constructs of A549 stably transfected cell lines with PGRN silencing/overexpression negative control for subcutaneous injection into nude mice, which were examined after tumor formation (28 d after transplantation). The results showed that the subcutaneous tumorigenic ability of nude mice was significantly weakened after PGRN silencing, and the volume and weight of solid tumors were significantly lower than those in the control group, whereas the volume and weight of solid tumors were significantly higher after PGRN overexpression than those in the control group (**Figure 4A-C**).

Expression of LncRNA H19 in NSCLC tissue and cells

qPCR was used to detect the expression of lncRNA H19 in tissue samples from 50 NSCLC patients and 10 healthy volunteers. The results showed that the expression of H19 was significantly higher in NSCLC tissue compared to that in healthy tissue (**Figure 5A**). The expression of H19 was detected in two NSCLC cell lines (A549 and 95D) and normal lung epithelial cells (DEAS-2B) using qPCR. The relative expression of H19 in A549 and 95D cells were higher than that in the normal lung epithelial cells (DEAS-2B) (**Figure 5B**). These results suggest that lncRNA H19 is closely associated with carcinogenesis and may be a pbiomarker for NSCLC.

LncRNA H19 promotes the proliferation, migration, and invasion of NSCLC cell lines

The expression of lncRNA H19 in A549 cells after plasmid and lentiviral transfection was detected by qPCR. After plasmid and lentiviral transfection, the expression of H19 was significantly increased in the H19 overexpression

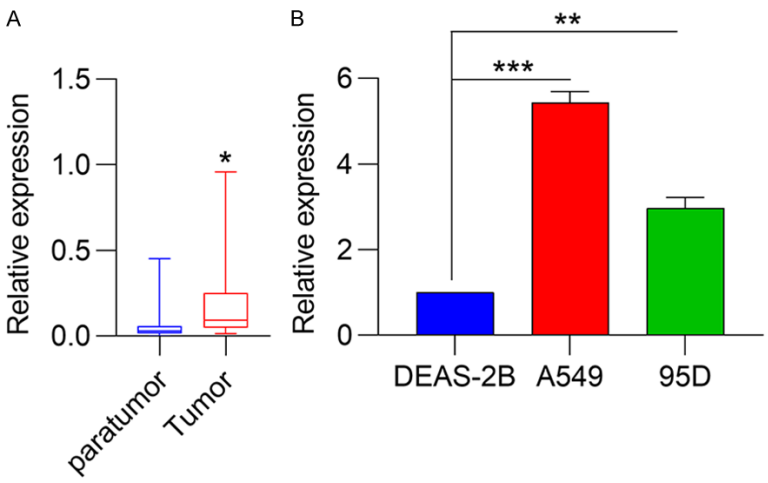

Figure 5. Comparison of H19 expression in non-small cell lung cancer tissue and cells with that in normal lung tissue and epithelial cells. A. qPCR detection of H19 expression in lung tissue from NSCLC patients (N = 50) and healthy volunteers (N = 10); B. qPCR detection of H19 expression in NSCLC cell lines and normal lung epithelial cells DEAS-2B. N = 3. **P < 0.01, ***P < 0.001.

group and decreased in the lncRNA H19 silencing group (**Figure 6A**, **6B**).

The effect of H19 on the proliferative ability of NSCLC cell lines was verified by CCK-8 proliferation and clone formation assays. Compared to that in the NC group, the cell proliferation activity of the LncRNA H19 group was significantly increased, peaking at 72 h (**Figure 6C**). However, compared to that in the NC group, the proliferative activity of the cells in the H19-silenced group was substantially reduced and was prominent in both groups (**Figure 6C**). In addition, the results of the clone formation assay showed that cell proliferation was significantly increased in the H19 overexpression group compared to that of the NC group. In contrast, cell proliferation was significantly decreased in the H19 silencing group compared to that in the si-NC group (**Figure 6D**, **6E**). Thus, lncRNA H19 promotes the proliferation of NSCLC cell lines.

The effect of H19 on cell cycle changes in NSCLC cell lines was examined using flow cytometry. The results showed that the duration of the G1 phase was significantly increased and that of the S phase was significantly reduced in the H19-interfered group compared to those in the control group. These results suggest that knockdown of lncRNA H19 expression can induce G1 arrest (**Figure 6F**).

The effect of lncRNA H19 on the migration and invasion abilities of NSCLC cell lines was verified using wound healing and transwell invasion assays. The results of the wound healing assay showed that the healing rate of the H19 overexpression group was significantly increased compared with that of the NC group. In contrast, the healing rate of the H19 interference group was significantly decreased compared with that of the si-NC group (**Figure 6G**). The results of the transwell invasion assay showed that the number of cells crossing the porous membrane of the H19 overexpression group was significantly higher than that in the NC group, whereas the number of cells crossing the membrane in the H19 silencing group was significantly lower than that of the NC group (**Figure 6H**). This indicates that H19 promotes the invasion of tumor cells.

LncRNA H19 promotes the proliferative activity of NSCLC cells in vivo

A tumorigenic assay on nude mice demonstrated that H19 boosted the proliferative activity of NSCLC cells in vivo. The results showed that the tumor growth rate, volume, and weight in the H19-silenced group were significantly reduced compared to those in the sh-NC group (**Figure 7A-C**). This indicated that H19 promoted the proliferation of NSCLC cells in vivo.

LncRNA H19/miR-29b-3p/PGRN shared a targeting relationship

Previous literature reported that there is a targeting relationship between H19 and microRNA (miR)-29b-3p [22-24], and between miR-29b-3p and PGRN [25, 26]. It has also been documented that the H19/miR-29b-3p/PGRN axis promotes epithelial-mesenchymal transition in colorectal cancer cells [22]. The dual-luciferase reporter gene assay showed that the fluorescence intensity was significantly decreased in the H19 wild-type vector + miR-29b-3p mimic group compared to that in the H19 WT vector +

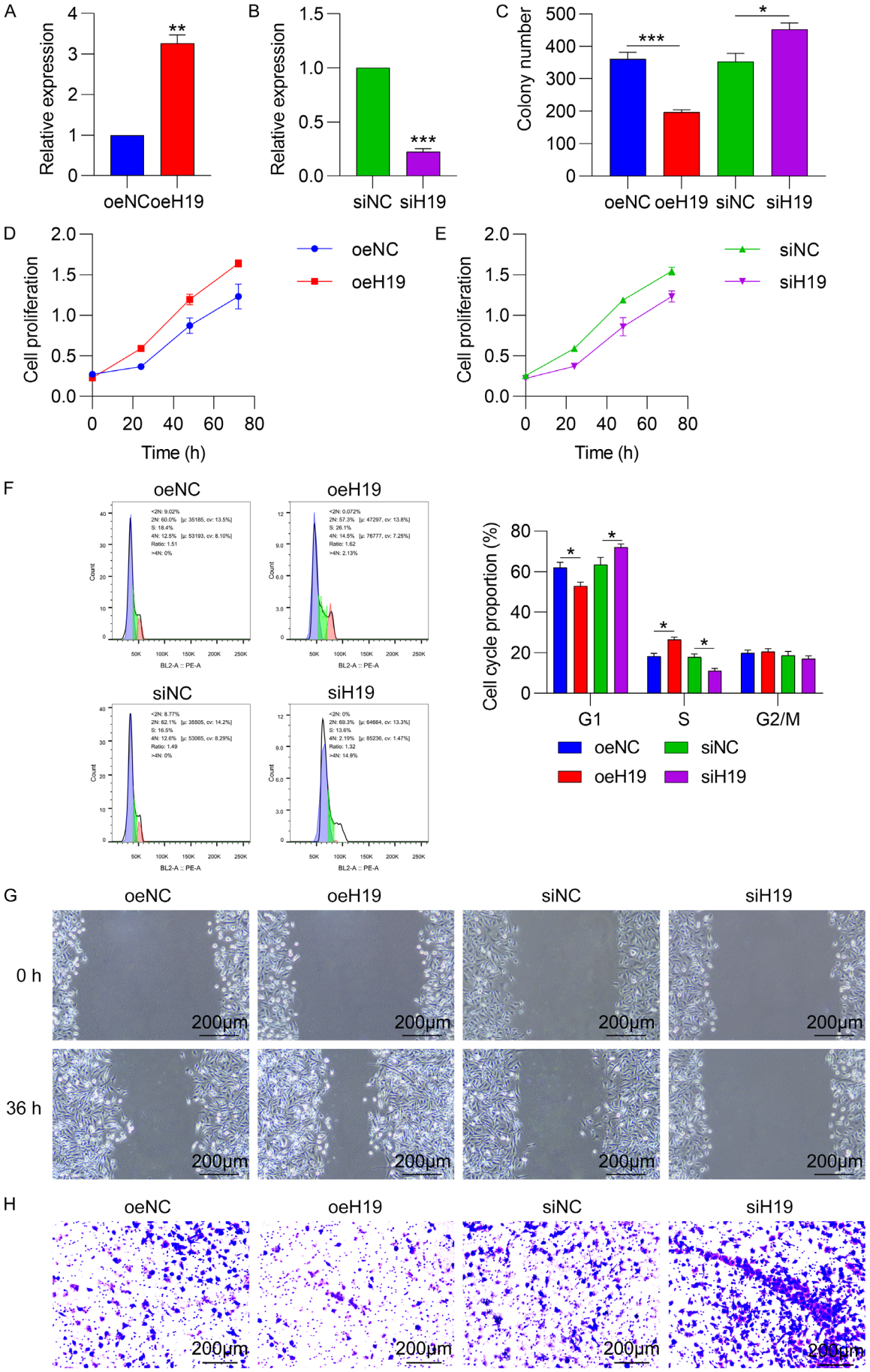
A
Relative expression
oeNC
oeH19
B
Relative expression
siNC
siH19
C
Colony number
oeNC
oeH19
siNC
siH19
D
Cell proliferation
Time (h)
oeNC
oeH19
E
Cell proliferation
Time (h)
siNC
siH19
F
oeNC
oeH19
siNC
siH19
Cell cycle proportion (%)
G1
S
G2/M
G
0 h
36 h
200μm
H

Figure 6. Effect of PGRN on proliferation, cell cycle, migration, and invasive activity of NSCLC cells. (A, B) qPCR detection of H19 expression in NSCLC cell lines after transfection with H19 overexpression plasmid and knockdown of siRNA; (C) CCK-8 assay for cell viability assessment; (D, E) Clone formation assay and detection of proliferation level of A549 cells; (F) Flow cytometry for cell cycle analysis; (G) Wound healing and (H) transwell assays to detect cell migration and invasive activity. N = 3. *P < 0.05, **P < 0.01, ***P < 0.001.

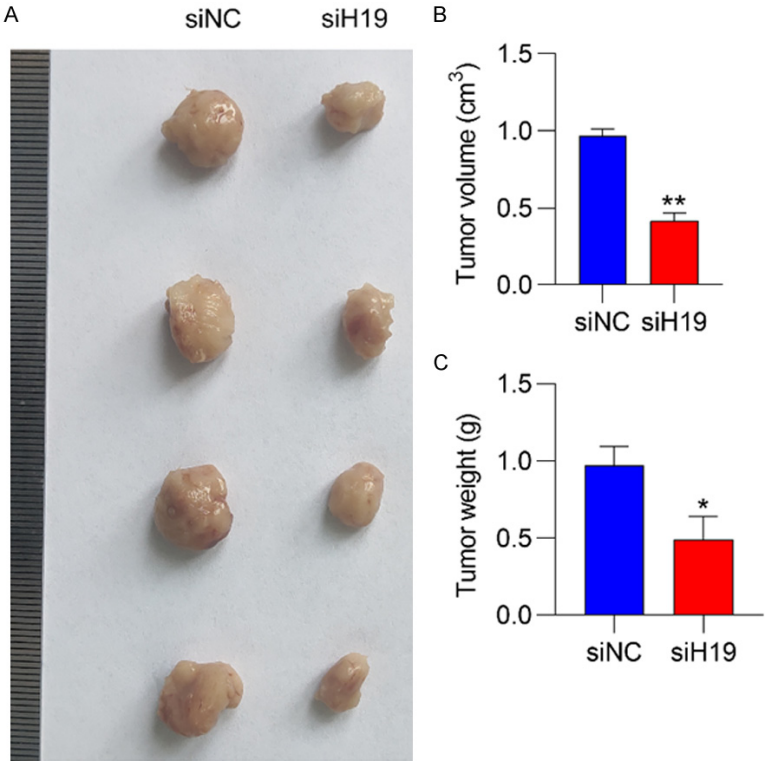

Figure 7. Effect of H19 on subcutaneous tumorigenic ability in nude mice. A549 stably transfected cell line silenced with H19 was constructed using a lentivirus for subcutaneous injection into nude mice, and was assayed after tumor formation. A. Representative tumor images; B. Tumor volume at 28 d after transplantation; C. Tumor weight. N = 5. *P < 0.05, **P < 0.01.

control mimic group (**Figure 8A**). Compared to that in the PGRN WT vector + control mimic group, the fluorescence intensity of the PGRN wild-type vector + miR-29b-3p mimic group was significantly decreased (**Figure 8B**). These findings suggest that H19 and miR-29b-3p, respectively have a targeting relationship to PGRN.

We used qPCR to confirm the relationships among the three genes, further elucidating their targeting relationship. First, we examined the expression of miR-29b-3p in NSCLC cell lines. The findings revealed that in contrast to H19, miR-29b-3p was expressed at lower levels in A549 and 95D cells than in healthy lung epithelial cells (**Figure 8C**). These results suggested that H19 may be involved in the development and progression of NSCLC by interacting with miR-29b-3p.

Next, we investigated whether H19 interacts with miR-29b-3p in NSCLC cells. We examined the expression levels of miR-29b-3p in cell lines stably overexpressing H19, in cell lines with knocked down H19, and in control cell lines, as well as the expression of H19 after overexpression or inhibition of miR-29b-3p. The results showed that the expression level of miR-29b-3p in the cell lines stably overexpressing H19 was lower than that in the control cell lines (**Figure 8D**), and the expression level of miR-29b-3p in the cell lines with H19 knockdown was higher than that of the control cell lines (**Figure 8E**). The expression level of H19 decreased after the overexpression of miR-29b-3p relative to that of controls (**Figure 8F**), and the expression level of H19 increased after the inhibition of miR-29b-3p expression (**Figure 8G**). This suggests that miR-29b-3p and lncRNA H19 interfere with each other.

The regulatory relationship between H19 and PGRN was examined using qPCR and WB. The qPCR and WB showed that H19 silencing significantly reduced the mRNA and protein expression levels of PGRN in NSCLC cells (**Figure 8H** and **8I**). Overexpression of H19 increased the mRNA and protein expression levels of PGRN (**Figure 8J** and **8K**). These results suggest that H19 plays a role in NSCLC development by upregulating PGRN expression.

Discussion

The incidence of NSCLC is on the rise owing to changes of environmental factors, lifestyle, and

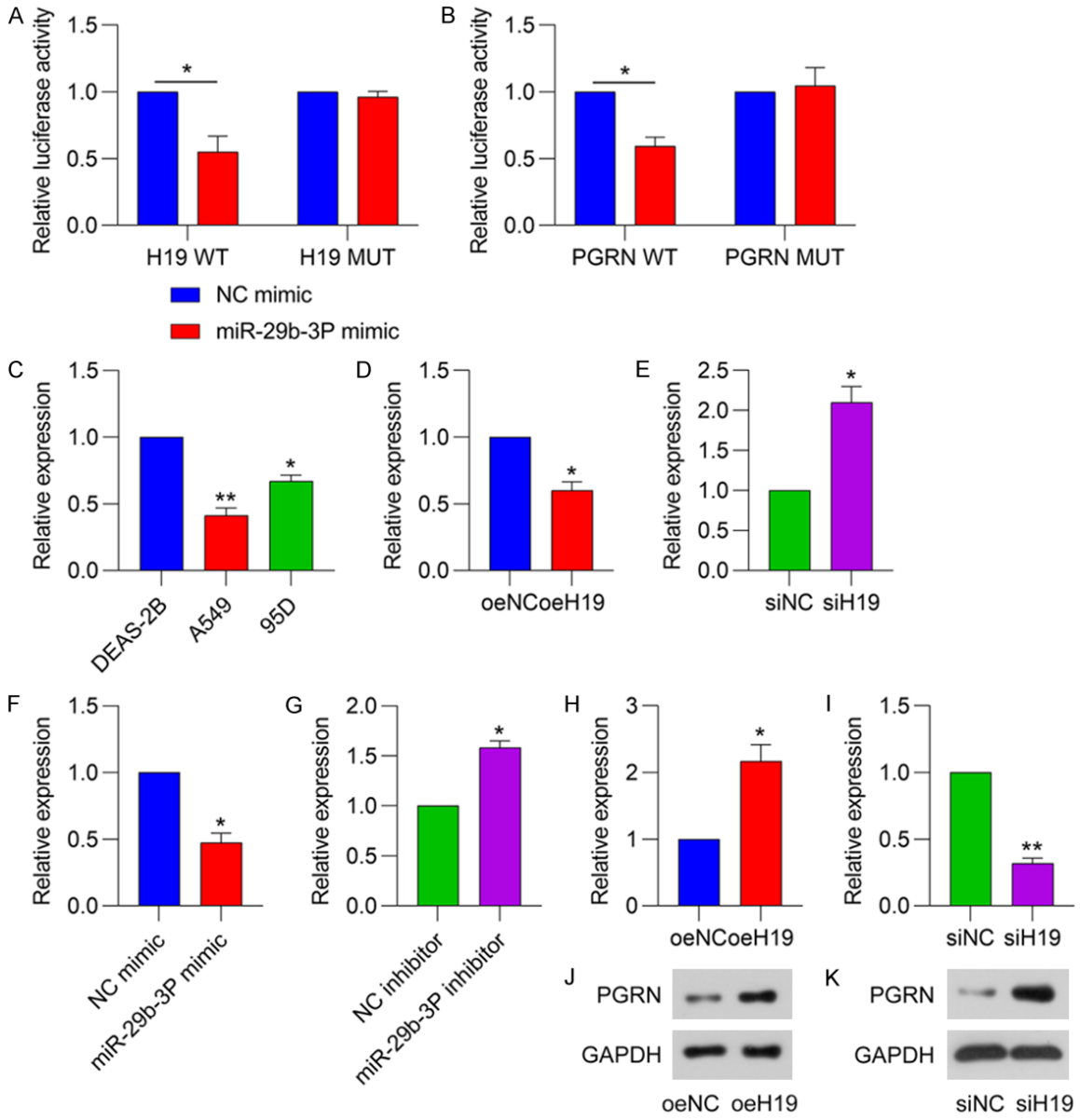

Figure 8. Relationship of H19 with miR-29b-3P and PGRN in NSCLC cells. A. Dual luciferase assay to detect the interaction of H19 and miR-29b-3P; B. Dual luciferase assay to detect the interaction of miR-29b-3P and PGRN; C. qPCR to determine the expression level of miR-29b-3P in A549 cells; D-G. miR-29b-3P inhibits the expression of LncRNA H19 in A549 cells; H, I. qPCR and WB assays in A549 cells with knockdown of H19 to regulate PGRN mRNA and protein expression; J, K. A549 cells overexpressing H19 showing regulation of PGRN mRNA and protein expression (qPCR and WB assays). N = 3. *P < 0.05, **P < 0.01.

dietary habits, and the 5-year survival rate is still below 50% [1, 27]. Therefore, it is crucial to investigate the intricate biologic pathways underlying NSCLC and to identify efficient biomarkers for disease diagnosis and management. Currently, there are no commonly used or clinically approved biomarkers for NSCLC. PGRN is expressed at high levels in a wide range of tumor cells, and the high levels are associated with poor prognosis. A growing number of studies have investigated the function of PGRN in tumors and discovered that it performs a variety of biological functions in tumor cells, including improving the efficacy of radiation therapy and chemotherapy, as well as encouraging cell migration and invasion [22, 28]. The role of PGRN has been demonstrated in breast, lung, and bladder cancers [29].

Additionally, PGRN affects cancer cells through a variety of signaling pathways and molecules, including Akt, VEGF, MAPK, and cell cycle protein D1 [30, 31]. A previous study showed that PGRN knockdown inhibited glioma cell growth [32]. Chen et al. [11] showed that PGRN expression was higher in male patients with lung adenocarcinoma than in those with lung squamous cell carcinoma, whereas no difference was observed in female patients. Overexpression of PGRN promoted the proliferation and anti-apoptosis of H520 (derived from lung squamous cell carcinoma) cells, whereas knockdown of PGRN inhibited the proliferation and anti-apoptosis of A549 (derived from lung adenocarcinoma) cells. These findings are partly consistent with our data. In the present study, we examined the expression levels of PGRN in 50 NSCLC tissues and 10 normal lung tissues. We found that PGRN was aberrantly expressed in NSCLC and was higher in cancer tissue than in normal tissue. Next, we analyzed the relationship between PGRN expression and clinicopathologic features, and the results showed that PGRN expression was significantly correlated with tumor size and stage. Additionally, clinical PGRN expression levels were higher in the patients at T3/T4 stage and clinical stages III-IV, suggesting that PGRN may be associated with the progression of NSCLC. This study demonstrated a critical function of PGRN in the development of tumors and its potential as a biomarker for diagnosis, treatment, and prognosis. Abnormally high PGRN expression in NSCLC tissue specimens has been shown to be closely associated with clinical characteristics of the tumor. Subsequently, we overexpressed and silenced PGRN in A549 cells. The data showed that the overexpression, rather than silencing, of PGRN promoted cell proliferation, viability, migration, and invasion. The role of PGRN in A549 cells is consistent with previous findings in H520 cells [11]. Blood et al. reported that PGRN was a key target of microRNA-588, leading to the suppression of migration and invasion in lung cancer [33]. However, we could not find detailed data for this report.

LncRNAs play a key role in tumor development by regulating the expression of protein-encoding genes at the transcriptional and post-transcriptional levels [29]. Numerous studies have shown that lncRNAs can be used as potential biological tumor markers and therapeutic targets. In this study, we discovered that lncRNAs H19 and PGRN are crucial for the growth of NSCLC. We also found that PGRN and lncRNA H19 are significantly expressed in NSCLC cell lines and cancer tissue, and that they can facilitate the growth, migration, and invasion of NSCLC. lncRNA H19 can regulate NSCLC development through the miR-29b-3p/PGRN axis. This implies that PGRN and H19 may serve as biomarkers as well as potential therapeutic targets for NSCLC. This study explored the mechanism of lncRNA H19/miR-29b-3p/PGRN as a pathway influencing the development of NSCLC. Moreover, H19 or PGRN may also regulate other factors to regulate the development of NSCLC, and the specific mechanism deserves further investigation. The solid association between PGRN and H19, as well as miR-29b-3p with PGRN, still needs further confirmation. Also, the number of mice in the animal experiments is small, so a larger number of animals is needed in future investigation.

Disclosure of conflict of interest

None.

Address correspondence to: Bin Ni, Department of Thoracic Surgery, The First Affiliated Hospital of Soochow University, 899 Pinghai Road, Suzhou 215006, Jiangsu, China. Tel: +86-0512-65223637; E-mail: szvipniu@163.com

References

[1] Zappa C and Mousa SA. Non-small cell lung cancer: current treatment and future advances. Transl Lung Cancer Res 2016; 5: 288-300.

[2] Pikor LA, Ramnarine VR, Lam S and Lam WL. Genetic alterations defining NSCLC subtypes and their therapeutic implications. Lung Cancer 2013; 82: 179-189.

[3] Chen Z, Fillmore CM, Hammerman PS, Kim CF and Wong KK. Non-small-cell lung cancers: a heterogeneous set of diseases. Nat Rev Cancer 2014; 14: 535-546.

[4] Mundra JJ, Jian J, Bhagat P and Liu CJ. Progranulin inhibits expression and release of chemokines CXCL9 and CXCL10 in a TNFR1 dependent manner. Sci Rep 2016; 6: 21115.

[5] Montoya A, Yepes L, Bedoya A, Henao R, Delgado G, Vélez ID and Robledo SM. Transforming growth factor beta (TGFβ1) and epidermal growth factor (EGF) as biomarkers of leishmania (V) braziliensis infection and early therapeutic response in cutaneous leishmaniasis: studies in hamsters. Front Cell Infect Microbiol 2018; 8: 350.

[6] Yu Y, Xu X, Liu L, Mao S, Feng T, Lu Y, Cheng Y, Wang H, Zhao W and Tang W. Progranulin deficiency leads to severe inflammation, lung injury and cell death in a mouse model of endotoxic shock. J Cell Mol Med 2016; 20: 506-517.
[7] Yang D, Li R, Wang H, Wang J, Han L, Pan L, Li X, Kong Q, Wang G and Su X. Clinical implications of progranulin in gastric cancer and its regulation via a positive feedback loop involving AKT and ERK signaling pathways. Mol Med Rep 2017; 16: 9685-9691.
[8] Farzi N, Yadegar A, Aghdaei HA, Yamaoka Y and Zali MR. Genetic diversity and functional analysis of oipA gene in association with other virulence factors among Helicobacter pylori isolates from Iranian patients with different gastric diseases. Infect Genet Evol 2018; 60: 26-34.
[9] Pormohammad A, Mohtavinejad N, Gholizadeh P, Dabiri H, Salimi Chirani A, Hashemi A and Nasiri MJ. Global estimate of gastric cancer in Helicobacter pylori-infected population: a systematic review and meta-analysis. J Cell Physiol 2019; 234: 1208-1218.
[10] Wang H, Sun Y, Liu S, Yu H, Li W, Zeng J, Chen C and Jia J. Upregulation of progranulin by Helicobacter pylori in human gastric epithelial cells via p38MAPK and MEK1/2 signaling pathway: role in epithelial cell proliferation and migration. FEMS Immunol Med Microbiol 2011; 63: 82-92.
[11] Chen S, Bie M, Wang X, Fan M, Chen B, Shi Q and Jiang Y. PGRN exacerbates the progression of non-small cell lung cancer via PI3K/AKT/Bcl-2 antiapoptotic signaling. Genes Dis 2021; 9: 1650-1661.
[12] Zhou C, Huang Y, Wu J, Wei Y, Chen X, Lin Z and Nie S. A narrative review of multiple mechanisms of progranulin in cancer: a potential target for anti-cancer therapy. Transl Cancer Res 2021; 10: 4207-4216.
[13] Han Li C and Chen Y. Small and long non-coding RNAs: novel targets in perspective cancer therapy. Curr Genomics 2015; 16: 319-326.
[14] Anastasiadou E, Jacob LS and Slack FJ. Non-coding RNA networks in cancer. Nat Rev Cancer 2018; 18: 5-18.
[15] Zhang P, Wu W, Chen Q and Chen M. Non-coding RNAs and their integrated networks. J Integr Bioinform 2019; 16: 20190027.
[16] Kung JT, Colognori D and Lee JT. Long noncoding RNAs: past, present, and future. Genetics 2013; 193: 651-669.
[17] Schmitt AM and Chang HY. Long noncoding RNAs in cancer pathways. Cancer Cell 2016; 29: 452-463.
[18] Wang Q, Cheng N, Li X, Pan H, Li C, Ren S, Su C, Cai W, Zhao C, Zhang L and Zhou C. Correlation of long non-coding RNA H19 expression with cisplatin-resistance and clinical outcome in lung adenocarcinoma. Oncotarget 2017; 8: 2558-2567.
[19] Zhang E, Li W, Yin D, De W, Zhu L, Sun S and Han L. Erratum to: c-Myc-regulated long non-coding RNA H19 indicates a poor prognosis and affects cell proliferation in non-small-cell lung cancer. Tumour Biol 2016; 37: 5653.
[20] Zhang Q, Li X, Li X, Li X and Chen Z. LncRNA H19 promotes epithelial-mesenchymal transition (EMT) by targeting miR-484 in human lung cancer cells. J Cell Biochem 2018; 119: 4447-4457.
[21] Xia B, Li H, Yang S, Liu T and Lou G. MiR-381 inhibits epithelial ovarian cancer malignancy via YY1 suppression. Tumour Biol 2016; 37: 9157-9167.
[22] Ding D, Li C, Zhao T, Li D, Yang L and Zhang B. LncRNA H19/miR-29b-3p/PGRN axis promoted epithelial-mesenchymal transition of colorectal cancer cells by acting on Wnt signaling. Mol Cells 2018; 41: 423-435.
[23] Lv M, Zhong Z, Huang M, Tian Q, Jiang R and Chen J. lncRNA H19 regulates epithelial-mesenchymal transition and metastasis of bladder cancer by miR-29b-3p as competing endogenous RNA. Biochim Biophys Acta Mol Cell Res 2017; 1864: 1887-1899.
[24] Liu L, Liu L and Lu S. lncRNA H19 promotes viability and epithelial-mesenchymal transition of lung adenocarcinoma cells by targeting miR-29b-3p and modifying STAT3. Int J Oncol 2019; 54: 929-941.
[25] Chen L, Li Q, Wang J, Jin S, Zheng H, Lin J, He F, Zhang H, Ma S, Mei J and Yu J. MiR-29b-3p promotes chondrocyte apoptosis and facilitates the occurrence and development of osteoarthritis by targeting PGRN. J Cell Mol Med 2017; 21: 3347-3359.
[26] Zhi L, Zhao J, Zhao H, Qing Z, Liu H and Ma J. Downregulation of LncRNA OIP5-AS1 Induced by IL-1β aggravates osteoarthritis via regulating miR-29b-3p/PGRN. Cartilage 2021; 13 Suppl: 1345S-1355S.
[27] Jonna S and Subramaniam DS. Molecular diagnostics and targeted therapies in non-small cell lung cancer (NSCLC): an update. Discov Med 2019; 27: 167-170.
[28] Dong T, Yang D, Li R, Zhang L, Zhao H, Shen Y, Zhang X, Kong B and Wang L. PGRN promotes migration and invasion of epithelial ovarian cancer cells through an epithelial mesenchymal transition program and the activation of cancer associated fibroblasts. Exp Mol Pathol 2016; 100: 17-25.
[29] Gijselinck I, Van Broeckhoven C and Cruts M. Granulin mutations associated with frontotem-

poral lobar degeneration and related disorders: an update. Hum Mutat 2008; 29: 1373-1386.
[30] Koo DH, Do IG, Oh S, Lee YG, Kim K, Sohn JH, Park SK, Yang HJ, Jung YS, Park DI, Jeong KU, Kim HO, Kim H, Serrero G and Chun HK; KB-SMC Colorectal Cancer Team. Prognostic value of progranulin in patients with colorectal cancer treated with curative resection. Pathol Oncol Res 2020; 26: 397-404.
[31] Zanocco-Marani T, Bateman A, Romano G, Valentinis B, He ZH and Baserga R. Biological activities and signaling pathways of the granulin/epithelin precursor. Cancer Res 1999; 59: 5331-5340.
[32] Bandey I, Chiou SH, Huang AP, Tsai JC and Tu PH. Progranulin promotes Temozolomide resistance of glioblastoma by orchestrating DNA repair and tumor stemness. Oncogene 2015; 34: 1853-1864.
[33] Blood CH and Zetter BR. Tumor interactions with the vasculature: angiogenesis and tumor metastasis. Biochim Biophys Acta 1990; 1032: 89-118.